A Comparison of Two Objective Analysis Techniques for Profiler Time–Height Data

FREDERICK H. CARR

School of Meteorology, University of Oklahoma, Norman, Oklahoma

PHILLIP L. SPENCER AND CHARLES A. DOSWELL III

NOAA/National Severe Storms Laboratory, Norman, Oklahoma

JEFFREY D. POWELL

Vandenberg Air Force Base, Vandenberg, California

(Manuscript received 20 January 1994, in final form 19 December 1994)

ABSTRACT

Two methods for objective analysis of wind profiler data in time–height space are proposed and compared. One is a straightforward adaptation of a procedure developed by Doswell for introducing time continuity into a sequence of spatial analyses. The second technique, named the correlation method, introduces a new rationale for selection of the Barnes filter parameter that is based on knowledge of the statistical structure of wind profiler data. The advantages and disadvantages of each method are discussed. It is noted that the correlation method, in principle, allows the deduction of consistent sampling intervals in time and space for the most dominant phenomena resolved by the data provided by a given atmospheric observing system. It is recommended that an objective analysis of wind profiler data be performed before single- or multiprofiler kinematic calculations are made.

In addition, it is shown that the positions of extrema in kinematic quantities computed from profiler triangles are relatively insensitive to the number of passes used in the analysis procedures. In fact, it is demonstrated that multipass Barnes-type schemes can overfit the original data, suggesting that a one-pass method may be preferable provided that the filter parameter is selected properly.

1. Introduction

The installation of the National Oceanic and Atmospheric Administration's Wind Profiler Demonstration Network (WPDN) over the central United States provides the opportunity to examine the evolution of the wind field and subsequent derived quantities on an hourly basis.[1] These data and derived products are commonly displayed on time-height cross sections representing, for example, 24 h of kinematic data throughout the troposphere. While simply viewing the raw or quality-controlled data does not require that all time–height "points" have an observation, use of line integral techniques (e.g., Schaefer and Doswell 1979) to obtain kinematic quantities requires that the time–height wind data for each profiler site involved in the calculation have a one-to-one correspondence in time and space.

There are several reasons why such a one-to-one correspondence is not present in the profiler data. (i) Wind measurements are made with respect to local ground level; thus, the data exist at different heights for each profiler site. (ii) Missing data in the vertical (e.g., owing to low signal-to-noise ratios) and in time (e.g., a site being temporarily out of commission) are common, causing gaps in the data. (iii) Quality control procedures may detect and eliminate erroneous or unrepresentative winds, resulting in additional gaps in the data. Interpolation techniques can be used to address each of the above problems, but how to "blend" these techniques in regions requiring both time and height interpolation is not obvious and the cumulative filtering properties of these procedures are not easily determined.

We therefore recommend that profiler time–height data be *objectively analyzed* at each site before being used in kinematic or additional calculations. The primary goal of this paper, then, is to compare two analysis methods that have been developed for this purpose. The objective analysis step not only brings about one-to-one correspondence and gap filling in a systematic manner, but also allows one to filter the data such that

[1] Six-minute data are available for research use.

Corresponding author address: Frederick H. Carr, School of Meteorology, University of Oklahoma, 100 E. Boyd Street, Norman, OK 73019.

the resulting analysis contains only the desired time and vertical length scales. The two approaches we present are both based upon the Barnes (1964) objective analysis method. This is appropriate for diagnostic studies in which the data are generally evenly distributed and allows the user to configure the desired filtering properties. The first approach is an application of the procedure presented in Doswell (1977) for analyzing space–time data. The second method takes advantage of the statistical structure of the profiler data to select the relative weighting of the data at different time and height distances from each analysis point.

These two methods are summarized in section 2. Section 3 describes the quality control we use before any application of profiler data is performed, shows examples of the two analysis methods, and examines the differences between them. An examination of the sensitivity of kinematic calculations to different analysis procedures is made in section 4 followed by concluding remarks in section 5.

2. Objective analysis methods

a. Doswell (1977)

In this approach, the filtering properties of Gaussian weighting functions are exploited in both space and time to produce an analysis that has "suitable" spatial and temporal continuity. Specifically, each gridpoint value is determined from

$$f_i = \frac{\sum_m w_{im} f_m}{\sum_m w_{im}}, \qquad (1)$$

where f is any scalar variable; subscripts i and m represent gridpoint and station locations, respectively; and the weight function w_{im} is given by

$$w_{im} = \exp\left(-\frac{R_{im}^2}{\lambda^2} - \frac{T_{im}^2}{\tau^2}\right). \qquad (2)$$

Here, R and T represent the spatial and temporal separation of a datum from the grid point and λ and τ are parameters that determine the filter response function. Note that R could be in one-, two- or three-dimensional space; in the application here, R represents vertical distance. Barnes (1973) has shown that the response function D corresponding to (2) is

$$D = \exp\left[-\lambda^2\left(\frac{\pi}{L}\right)^2 - \tau^2\left(\frac{\pi}{P}\right)^2\right], \qquad (3)$$

where L is the wavelength and P is the period. In general, the parameters λ and τ are determined by specifying the response one desires at certain wavelengths and periods. These selections often are made with respect to the average spatial (Δs) and temporal (Δt) separation of the observations.

For example, one could require that the response D at the Nyquist wavelength ($L = 2\Delta s$) and period ($P = 2\Delta t$) be e^{-1}. Assuming that one desires the smoothing in time with respect to the Nyquist frequency to be the same as the smoothing in space with respect to the Nyquist wavelength (e.g., the response at $8\Delta s$ is the same as for $8\Delta t$), we obtain $\lambda \cong 0.45\Delta s$, $\tau \cong 0.45\Delta t$. It should be noted that this particular choice of λ and τ allows considerable small-scale information to be retained in the analysis (see Fig. 1). If derivative fields are to be computed, stronger smoothing of the smaller scales may be desired. Using the guideline that derivatives of quantities for wavelengths less than $6\Delta s$ are not well estimated (Doswell and Caracena 1988), Fig. 1 also shows the response (short-dashed line) for a choice of $D = e^{-1}$ at $L = 6\Delta s$, $P = 6\Delta t$ (this yielded $\lambda \cong 1.35\Delta s$, $\tau \cong 1.35\Delta t$). Note that the response is near 0 at $2\Delta s$, $2\Delta t$ while having a value of 0.698 at $10\Delta s$, $10\Delta t$. The response can be "sharpened" (i.e., kept near 0 at $2\Delta s$ while bringing the response at $10\Delta s$ toward unity) by performing two or more passes of the analysis, as outlined by Barnes (1964), Koch et al. (1983), and Achtemeier (1989).

Computational expense can be reduced by selecting "influence radii" in space and time—that is, by setting maximum values of R and T in (2). For example, values of R, $T = 5\Delta s$, $5\Delta t$ yield a weight of just 1.2×10^{-12} when $\lambda = 1.35\Delta s$ and $\tau = 1.35\Delta t$. However,

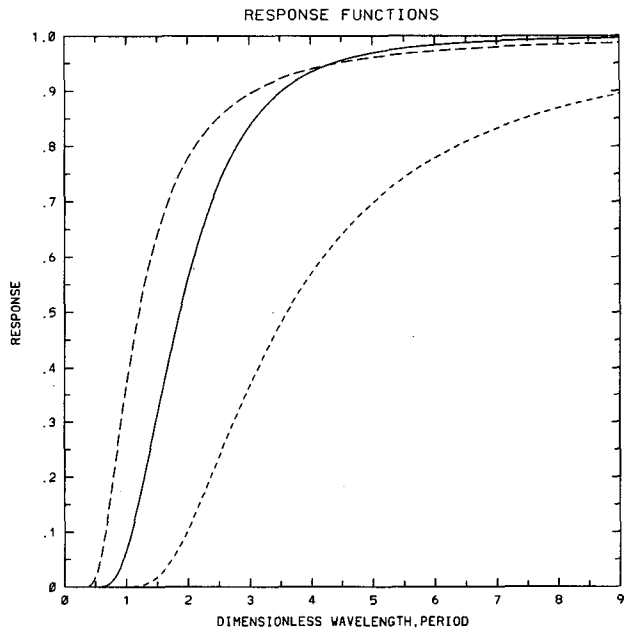

FIG. 1. Plots of two-dimensional response functions used in this study. The long-dashed line is for a one-pass scheme with $\lambda = 0.45\Delta s$, $\tau = 0.45\Delta t$. The short-dashed curve is also for a one-pass analysis but for $\lambda = 1.35\Delta s$, $\tau = 1.35\Delta t$. The solid line is for a two-pass scheme with $\gamma = 0.3$ and $\lambda = 1.35\Delta s$, $\tau = 1.35\Delta t$. The abscissa is both a dimensionless wavelength ($L/2\Delta s$) and period ($P/2\Delta t$).

they should be large enough so that at least several observations are within reach of grid points in the middle of small data-void areas.

The mean values used for Δs and Δt derived from the profiler data used here are 260 m and 1 h, respectively. Although the vertical gate spacing or sampling interval for the wind profiler is 250 m, the occasional missing or rejected observation leads to the value of 260 m.

b. *Use of correlation structure*

This method is motivated by the desire to determine the appropriate weighting of observations in the vertical to use in the analysis for a grid point, given that a specified weighting of data in time is to be used. The basic philosophy is *to design the Barnes weight function such that equal weight is assigned to equally correlated data in the vertical and in time.* This approach uses just the spatial part of (2) and knowledge of the statistical structure of profiler data is required to create the necessary "time-to-space conversion."

The correlation data used for this study are obtained from the work of Brewster and Schlatter (1988) and are shown in Figs. 2 and 3. These results are derived from over 22 000 observations taken from a 50-MHz wind profiler in Fleming, Colorado, during June 1987. The background (mean) field for the correlation calculation was a 24-h running mean of the data at each level, which were smoothed to eliminate scales of 200 m or less. Figures 2 and 3 show contours of the correlation in the vertical and in time, respectively, of the u component of the wind as a function of height. The time correlation (autocorrelation) results suggest a midtropospheric periodicity of 2–2.5 days for this data sample. In general, the midtropospheric data are more correlated in both time and vertical depth than are lower atmospheric and jet stream/tropopause levels. According to Brewster and Schlatter, the v-component correlation plots are similar to the u-component ones. It is important to note that we are using these data only to demonstrate our proposed technique; new correlation structures may need to be determined from the appropriate profiler sites and season before this method is used in future diagnostic studies. (Note that the sensitivity studies needed to determine just how frequently the statistics should be computed have not been performed here. In addition, a small sensitivity may appear as a result of the sampling differences between the 50-MHz and WPDN 404-MHz profilers.)

To illustrate our use of these data, we can see that at 5600 m MSL, for example, data 1600 m apart in the

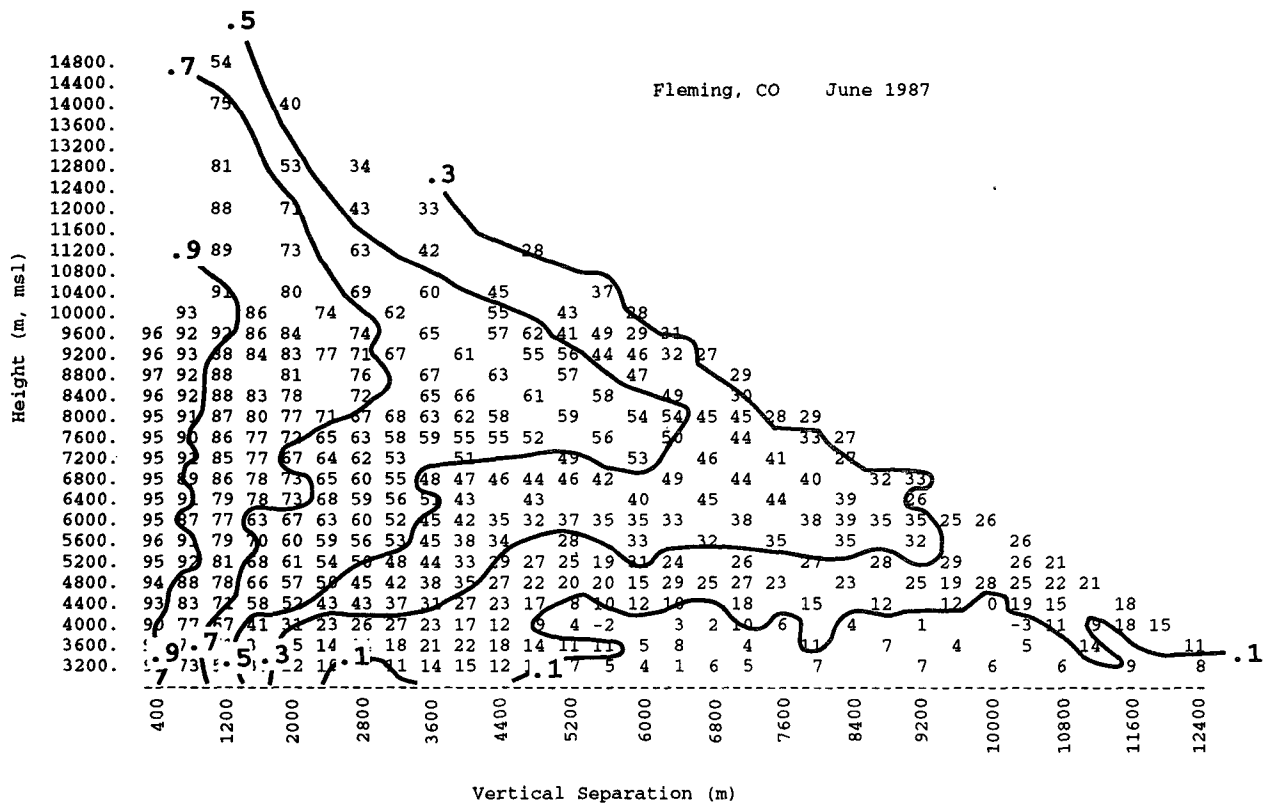

FIG. 2. The u-component correlations (×100) for the Fleming, Colorado, profiler during June 1987 as a function of height and vertical separation (after Brewster and Schlatter 1988).

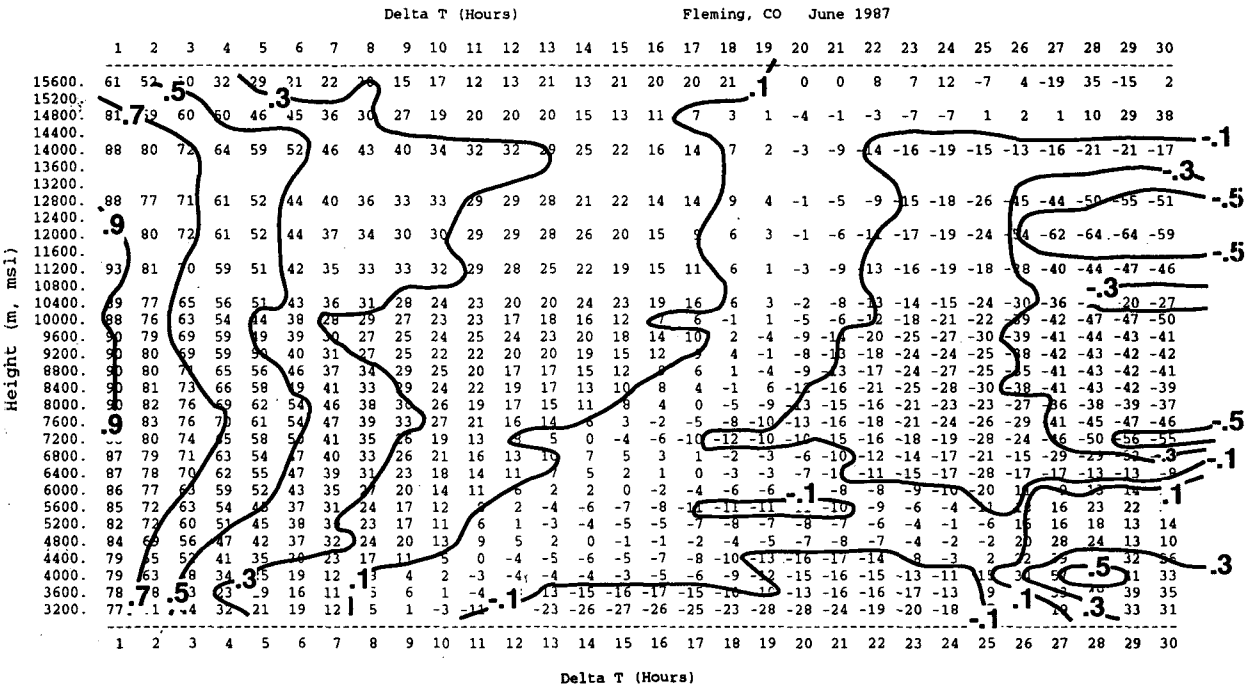

FIG. 3. The u-component correlations ($\times 100$) for the Fleming, Colorado, profiler during June 1987 as a function of height and temporal separation (after Brewster and Schlatter 1988).

vertical have the same correlation (0.70) as data separated by about 2.3 h in time. Hence, 1 h corresponds to a 696-m vertical separation at this level. Thus, we define the "time-to-space conversion factor" such that if 1 h is to be used as the mean sampling interval in time, then 696 m (according to this dataset) should be used as the corresponding Δs (mean vertical separation) at this level to ensure time–space consistency in the analysis.

The "time-to-space conversion factor" can be computed at as many levels as desired for a given correlation value. We computed the conversion factor every 800 m from the Brewster–Schlatter data using correlations of 0.70 and 0.50 (Fig. 4). Although variations between the two correlations exist at individual levels, the general pattern is similar. We somewhat arbitrarily selected the 0.70 values for use in the remainder of this work; however, it is clear from Figs. 2 and 3 that values greater than 0.80 and less than 0.30 are inappropriate because they do not extend through the full height range of the data.

Use of a different conversion factor with height ensures that the equal weight for equal correlation philosophy holds at each level. This is especially desirable if there is a large vertical variation in the conversion factor brought about, for example, by large differences between lower and upper tropospheric structure in a region. However, this also means that a different response function applies at each level. If it is important to the user that the analysis response be the same over the domain, or if the vertical variation of the conversion factor is small, a vertically averaged conversion value may suffice. For simplicity in presenting the differences between the two analysis methods proposed here, we use a constant value of 1 h = 749 m (computed from the 0.70 correlation values and shown in Fig. 4) for the remainder of this paper. Since the mean conversion value from the 0.50 correlation data is 710 m, no significant analysis differences arise between use of the mean 0.70 or 0.50 correlation curve data. A greater sensitivity results when performing analyses using the extremes (480 and 1080 m) present in the 0.70 data (see Fig. 4). The differences (not shown) are smaller than the differences to be shown between the two analysis approaches proposed here, and do not change the physical interpretation of the kinematic calculations; however, they are significant enough to indicate that retaining the vertical variation of the conversion factor may be of value in some cases.

The vertically averaged conversion factor is now the Δs value in the determination of λ. Time increments between the data and a grid point are first converted to "distances." The data in the z–t plane are then objectively analyzed in the same way as a typical data field in the x–y plane, with R in (2) varying in both directions and the time term absent. (Note that we could just as easily have used the time term only and converted vertical distances to time.) The response function for this analysis is also the short-dashed line in Fig. 1 (assuming λ is also $1.35\Delta s$); what has changed is that the

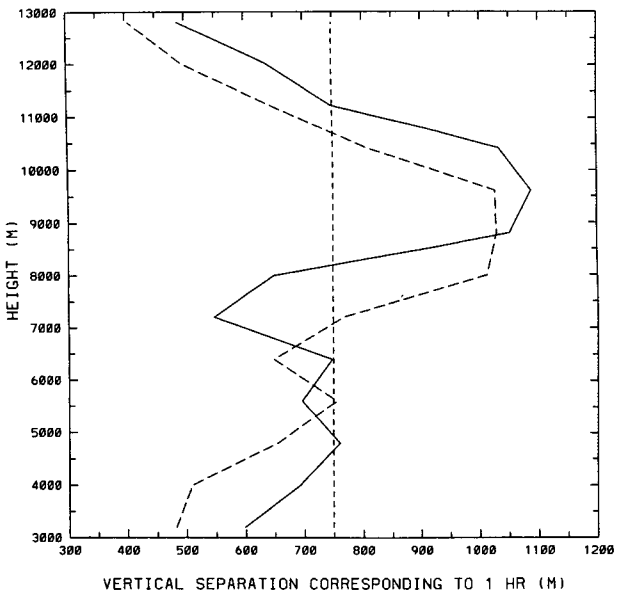

FIG. 4. The vertical separation (m) of profiler data that has the same correlation as data 1 h apart, computed from the Brewster–Schlatter correlation tables using the 0.70 correlation curve (solid line) and the 0.50 correlation curve (long-dashed line), plotted as a function of height (m). The short-dashed line is the vertical mean of the 0.70 values.

Δs used to compute the dimensionless wavelength is now 749 m rather than the 260-m mean vertical separation computed from the profiler data.

3. An example

a. *Quality control*

Although manual quality control (QC) of wind profiler data can be done quickly by someone experienced in profiler system characteristics, it is desirable to have an automated procedure so that the same quantitative criteria are applied to all time–height sections. The purpose of our QC algorithm is to detect data that are clearly erroneous or unrepresentative. No pretense is made that the procedure described here is "objective," since it has subjectively chosen thresholds and criteria that are consistent with the specific purpose of the editing. For example, the QC of profiler data to be used in derivative calculations should be more strict than the editing done at NOAA's Profiler Hub (Brewster 1989), which removes only the most flagrantly bad data and allows users to make their own judgements on the remaining data.

Table 1 summarizes the procedures used in this study. These checks are derived primarily from the work of Brewster and Schlatter (1986) and Brewster (1989). The QC is done separately for the u and v components of the wind (except during speed and directional shear checks). If either of the components is rejected, then the other component is also eliminated. No attempt is made to correct data. We perform the QC in research or "two-sided" mode; that is, the data used are centered in time with respect to the checked point rather than using the one-sided in time QC necessary for real-time operations. A brief discussion of Table 1 is given below; a more complete description of the QC procedure is given by Spencer (1992).

Two median checks, "large" and "small," are done first and second, respectively. The large median check, involving up to 150 data values in a 6 h × 6 km "box," can remove small areas of well-correlated errors that are embedded within good data, while the small median check is useful in eliminating single points sufficiently different from their neighbors. If the difference between a datum's value and the median of the large or small box is greater than a specified threshold value, the datum is removed. Two threshold values, T1 and T2, are computed. As shown in Table 1, T1 is derived from a quadratic whose coefficients are selected by the user to allow different thresholds with height. For the June dataset used in the example, we specified 9.5 m s^{-1} at the surface, 17.0 m s^{-1} at 9000 m, and 14.0 m s^{-1} at 16 000 m (following Brewster and Schlatter 1986). The second threshold, T2, is based only on wind speed. The parameter SPEED in Table 1 is the average of the observed wind component and the median value.

TABLE 1. Summary of quality control procedures.

Median checks	
Large median check	Small median check
use 6 h × 6 km "box"	use data closest to center point in each of 8 directions (but within large "box")
T1 = $a(Ah^2 + Bh + C)$	T1 = $b(Ah^2 + Bh + C)$
T2 = 0.4(SPEED)	T2 = 0.4(SPEED)
a usually ≥ 1	b usually ≤ 1
Threshold = max (T1, T2)	
1 pass through data	2 passes through data

Shear checks		
Directional shear		Speed shear
Separation (S)	Allowable shear	
$S < 300$ m	25°	if $\frac{\min(\text{mag1, mag2})}{\max(\text{mag1, mag2})} \leq 0.5$,
300 m $< S <$ 600 m	30°	remove datum at level 2 if
600 m $< S <$ 1 km	40°	$\frac{\min(\text{mag1, mag3})}{\max(\text{mag1, mag3})} \geq 0.8$
1 km $< S$	no test	

Allowable shear can also be a function of wind speed.
Multiple passes are optional.

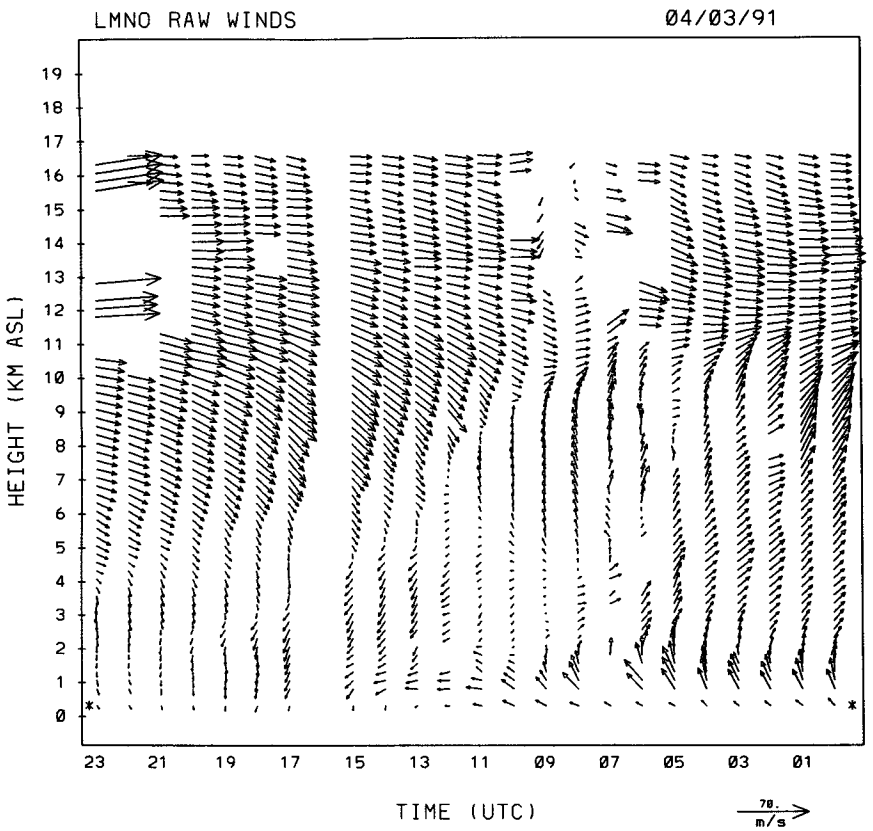

FIG. 5. Observed winds from the Lamont, Oklahoma, profiler site on 3 April 1991. The asterisk marks the ground level.

The threshold used in the median checks is the *larger* of T1 and T2. In regions of high wind speeds, T2 is usually larger than T1 and thus prevents the rejection of legitimate jet stream winds.

The parameters a and b in the T1 formulas enable the user to create a "strict" or "lenient" QC. Small values of a and b will eliminate more data. In our experience, a value of 2.0 for a and values between 0.5 and 1.0 for b produced the best compromise that prevents the elimination of good winds and retention of bad ones. (The decision on what are "good" and "bad" winds is ultimately subjective, and is based here on synoptic judgement and knowledge of the characteristic sources of errors in profiler data.) One can also make more than one pass through the data, as the median changes when data are eliminated. One pass is usually sufficient for the large median check while two passes have been found beneficial for the small median check.

Speed and directional shear checks can detect unrepresentative data not found by the median checks. The shear checks compare adjacent winds in the vertical, with the rejection decision determined by the next adjacent or third wind. The rejection criteria shown in Table 1 are values we have used successfully but could be modified for other datasets. The directional shear check could be made a function of wind speed if one wants to allow greater variation in wind direction under light wind conditions (or less variation in a jet stream environment). Multiple passes of these shear checks also can be made, although we did not do so here.

b. Results

Figure 5 is the raw wind profiler data from Lamont, Oklahoma, for 3 April 1991. A surface low passed to the south of Lamont around 1200 UTC. The low remained closed off for 5–6 km in the vertical and then opened up as an "eastward-tilting" wave (assuming a time-to-space conversion is valid) at higher levels. This case is examined in some detail by Spencer (1992). Both median and shear checks are performed, with parameters a and b equal to 2.0 and 0.6, respectively. The number of rejected values is 26 (see Fig. 6), which represents just 2% of the data. The eliminated data are either clearly bad or are unrepresentative in their local area. [The low-level wind maxima from 0000 to 1300 UTC in Fig. 5 could possibly be migrating bird contamination (Wilczak et al. 1995), but an inspection of the original returned power and spectral width data and

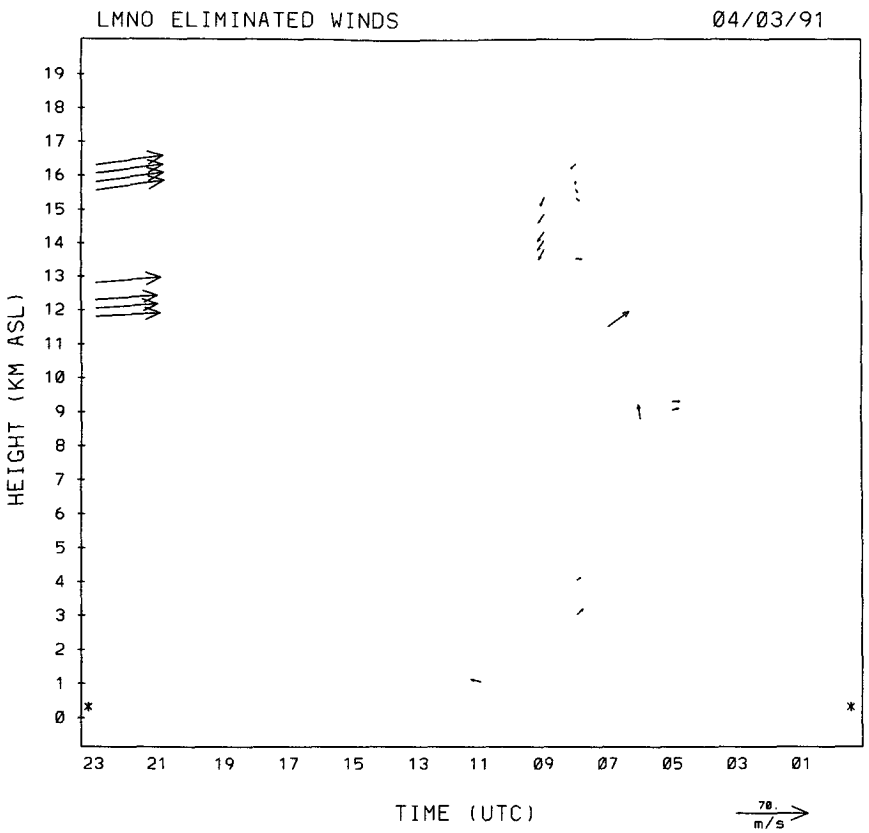

FIG. 6. Lamont profiler winds rejected by the quality control procedures. The asterisk marks the ground level.

nearby rawinsonde data supports the existence of an actual low-level jet at this time.] Since the median checks are done first, they typically remove the most data, about two-thirds in this case. Note that the QC does not eliminate "small-scale" features in the data. The user can control the retention or elimination of such features via the design of the objective analysis weight function.

Objective analyses of Lamont's quality-controlled winds are performed using both analysis methods (Fig. 7). Figure 7a is the one-pass Doswell (1977) analysis with $\Delta s = 260$ m, $\Delta t = 1$ h, $\lambda = 1.35\Delta s$, and $\tau = 1.35\Delta t$ (the response function for this is the short-dashed line in Fig. 1.) Although this choice of λ and τ represents significant filtering of vertical scales shorter than 1.5 km and temporal scales less than 6 h, the essential features of this dataset (e.g., the low-level jet and veering winds ahead of the low, the 5-km-deep easterly flow at 1100–1200 UTC and the tilted upper trough) are well represented. The root-mean-square (rms) differences between the Lamont quality-controlled winds and the analyzed winds bilinearly interpolated back to the observation points are 1.1 and 1.3 m s^{-1} for the u and v components, respectively. These are close to the expected accuracy of wind profiler measurements (e.g., see Strauch et al. 1987). Thus, the above choice of parameters forces the analysis to conform to the data only to the degree of the accuracy of the data itself.

The analysis from the correlation method (Fig. 7b) results in greater smoothing in the vertical. The u and v rms differences here are 1.7 and 1.9 m s^{-1}, respectively. Further discussion of the differences between the two methods is contained in the following section.

c. *Comparison of the two methods*

The primary difference between the two objective analysis methods described here is how the filtering parameter(s) in the Barnes analysis are selected. In the Doswell (1977) approach (denoted as D77 for the remainder of this discussion), the parameters are related to the mean sampling intervals in space and time. It is implicitly assumed that the atmosphere is marginally sampled and the objective is to design the analysis weights such that the minimum wavelength in each direction (time and space) that is measured reliably is preserved in the analysis. In the correlation method, a calculation is first made, using the results from wind profiler time and height correlation tables, that shows

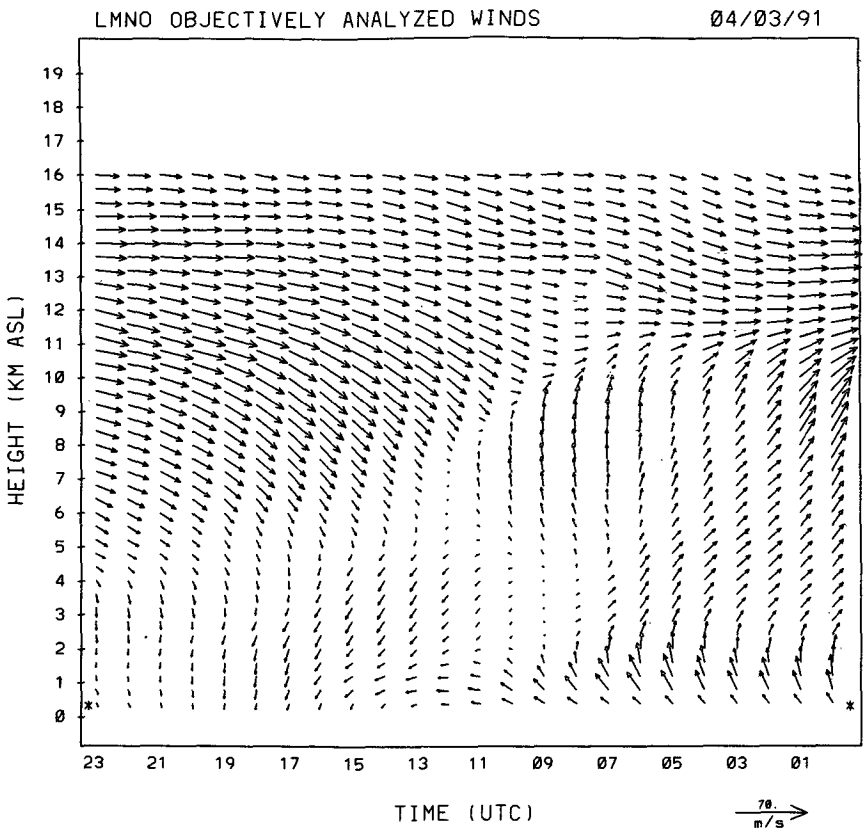

FIG. 7. Objective analysis of the Lamont profiler winds on 3 April 1991. (a) Using the Doswell (1977) method. (b) Using the correlation method. The asterisk marks the ground level.

what the "mean separation" in one direction should be, given what the mean sampling interval is in the other direction. Thus, observed atmospheric structure determines the proper choice for analysis parameters, not the chosen sampling interval of the instrument. This procedure seeks consistency in the weighting of equally correlated data.

Significant differences between the two methods will arise only if one direction in time or space is sampled much more frequently than another. To illustrate this, we show a two-dimensional plot in $z-t$ space of the two weight functions determined for the analysis of the 2–3 April 1991 profiler data (Fig. 8). Since the correlation method allows one to compute an equivalence between vertical and temporal separation, the ordinate in Fig. 8, representing vertical separation, is spaced such that the weight function contours determined from the June 1987 data (dashed lines) appear circular. The solid lines outline the weights for the D77 scheme, also for hours ± 1 to ± 4, when λ, $\tau = 1.35\Delta s$, $1.35\Delta t$, respectively, $\Delta s = 260$ m and $\Delta t = 1$ h. One can see that, owing to the small mean sampling interval, the D77 method assigns less weight to data at a given vertical distance than does the correlation method. As sampling intervals change, so will the shape of the D77 weights, while the weights for the correlation method will stay the same. On the other hand, weights for the correlation method may be geographically and seasonally dependent and thus should be redetermined depending on when and where the case study of interest occurred. It is anticipated that in a strong jet stream regime, for example, the correlation in time (vertical separation) would increase (decrease) relative to that seen in the June data presented in Figs. 2 and 3.

The vector difference field was computed between the D77 and correlation method analyses for the Lamont 3 April 1991 data (Fig. 7a minus Fig. 7b; see Fig. 9). The subtraction of one filtered field from another results in a bandpass filter of the data and emphasizes those scales where the difference between the two filters is greatest. The result here shows the small-scale vertical structure that was incorporated into the D77 analysis that is not present in the correlation method analysis. Figure 9 is thus consistent with the implications of Fig. 8; that is, since the D77 weights decrease more rapidly with height, less vertical smoothing occurs. For example, the vertical shear in the low-level jet between 0000 and 0900 UTC is larger in the D77 analysis. However, it is not known to what extent all

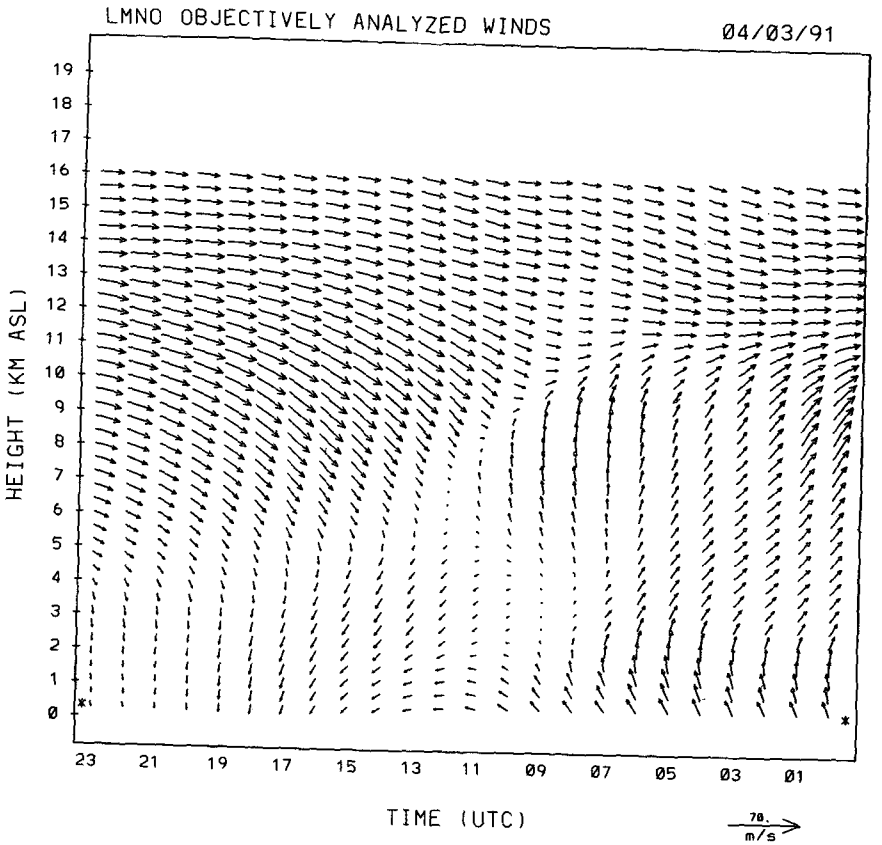

FIG. 7. (*Continued*)

of the tropospheric small-scale structure shown in Fig. 9 is desired in the analysis; this depends on the objectives of the study and the signal-to-noise ratio in the data.

4. Sensitivity of kinematic calculations

It is important in diagnostic studies of atmospheric structure to know how the response function of the objective analysis procedure used affects the results. It often is tempting to make full use of the maximum spatial and/or temporal resolution provided by an observing system. The multipass objective analysis procedures described by Barnes (1964), Koch et al. (1983), and Achtemeier (1989) outline how to obtain a significant response at scales just above $2\Delta s$, $2\Delta t$ while maintaining a small response at these Nyquist scales. Here we provide an example of the sensitivity of kinematic quantities derived from wind profiler data to the response functions from one- and two-pass Barnes schemes.

The weight function for the second pass of a z–t Barnes analysis can be written as

$$w_{im} = \exp\left(-\frac{R_{im}^2}{\gamma\lambda^2} - \frac{T_{im}^2}{\gamma\tau^2}\right), \qquad (4)$$

where γ is an empirical factor used to accelerate convergence toward a particular idealized response. The final response for the two passes, as shown by Barnes (1973), is given by

$$D_1^* = D_0(1 + D_0^{\gamma-1} - D_0^{\gamma}), \qquad (5)$$

where D_0 is the response of the first pass [Eq. (3)]. If, for example, the objective is to examine the profiler data for plausible small-scale features, γ can be set to 0.2 and λ determined by requiring that the final response at the Nyquist wavelength be e^{-1} (see Koch et al. 1983). This yields an 85% response for $4\Delta s$, $4\Delta t$ scales, which confirms that this two-pass procedure does indeed retain much small-scale amplitude.

A two-pass analysis using these choices of γ and Nyquist response is performed on the quality-controlled Lamont data. The result (not shown) yields an analysis that looks nearly identical to the input data (Fig. 5 minus the eliminated winds shown in Fig. 6). The rms differences for both the u and v components are about 0.3 m s^{-1}. This is fitting the data more closely than can be justified by the estimated accuracy of the data. Thus, while one might desire to design an analysis procedure whose response conforms closely to an "ideal" filter (i.e., a sharp cutoff between measured and unmeasured scales), it may result in overfitting

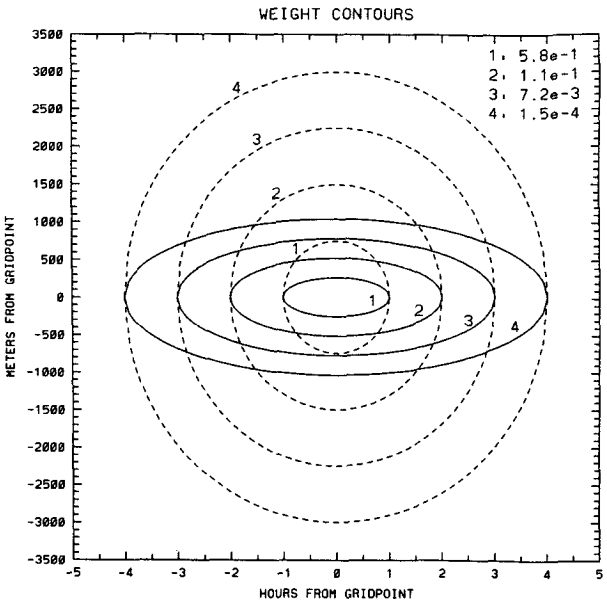

FIG. 8. Plot of the two-dimensional weight functions used in the Doswell (1977) (solid lines) and correlation method (dashed lines) analyses. The contour values for each set of four lines are given in the upper-right corner.

unreliable small-scale features in the data, depending on how the parameter choices have been made.

We now show kinematic quantities resulting from two additional, more conservative analysis procedures applied to wind profiler triangles. The first is a two-pass application of the D77 procedure used in section 3 to produce Fig. 7. Recall that with $\lambda = 1.35\Delta s$ and $\tau = 1.35\Delta t$, we have a D_0 response of e^{-1} at $6\Delta s$ and $6\Delta t$ scales. With $\gamma = 0.3$, the two-pass analysis yields a $D_1^* = 0.836$ response at $6\Delta s$, $6\Delta t$ (but still only a $D_1^* = 0.067$ response at $2\Delta s, 2\Delta t$). The complete two-pass response is given by the solid line in Fig. 1.

The second analysis is the one-pass D77 procedure used to obtain Fig. 7a. Both analyses are performed on 48 h of quality-controlled data from a Vici–Lamont–Purcell wind profiler triangle over the western half of Oklahoma for the 2–3 April 1991 period. The procedure for the computation of divergence and vorticity is a slightly modified version of the Schaefer and Doswell (1979) method as presented by Zamora et al. (1987) and is summarized in appendix A. Vertical motion is computed from divergence adjusted such that its vertical integral sums to zero and with vertical velocities assumed to be zero at the surface and 150 mb. All kinematic quantities are computed and displayed with pressure as the vertical coordinate; the equivalence between height and pressure is obtained from nearby radiosonde data.

Vorticity and vertical motion time–height sections are computed from winds analyzed by the two-pass D77 procedure (Fig. 10). Considerable detail is present in both fields. There is a good correspondence between the cloud cover, current weather, and 3-h precipitation amounts shown in Fig. 10b and the computed vertical motion. Despite the more conservative choices for γ and the Nyquist response, the average rms fit to the u and v components from the three profilers is near 0.5 m s^{-1}, still a smaller value than justified by the accuracy of the observations. Even a two-pass procedure with $\gamma = 1$ fits the data to within 0.9 m s^{-1}.

The vorticity and vertical motion fields computed from the one-pass analysis (where the rms fit was near 1.2 m s^{-1}) are smoother, with the maxima and minima having reduced amplitudes (Fig. 11). However, the phases of the major extrema in the one-pass results have not shifted in time or height from the two-pass centers. (Appendix B explains why this is so.) Thus any physical interpretation of the results remains unchanged. The same fields computed using the one-pass correlation method that produced Fig. 7b are shown in Fig. 12; note that the vertical structure, as expected, is even smoother than for the one-pass D77 method but the extrema are still in the same locations. Use of different time-to-space conversion factors from Fig. 4 caused about a 10% change in the results (not shown), primarily related to details in the vertical structure; the basic pattern remained unchanged.

5. Discussion

We have presented two ways to approach the objective analysis of time–height cross section data. The concepts discussed here, however, can be applied to any two-, three- or four-dimensional application of a Barnes-type analysis scheme. We begin by recommending the use of a distance-weighting analysis method for wind profiler time–height data in order to (i) align data from different profiler sites to a common z–t grid for subsequent multiprofiler calculations; (ii) fill in data gaps without resorting to one-dimensional interpolation techniques that are sensitive to the few points used on each side of the gap; and (iii) filter the data in a user-specified manner consistent with data sampling intervals and the goals of the application.

Both techniques use the Barnes (1964) weight function, and one is a straightforward adaptation of the Doswell (1977) procedure for introducing time continuity into a sequence of spatial analyses. The second technique, however, introduces a new rationale for selection of the Barnes filter parameter that is based on knowledge of the statistical structure of wind profiler data. These methods were presented and compared in sections 2 and 3. Here we will summarize in the context of what are the advantages and disadvantages of each technique and how a user would select one or the other for a particular application.

The D77 procedure is appropriate when one seeks the maximum *allowable* detail in each sampled direction. The Barnes filter parameters are a function only

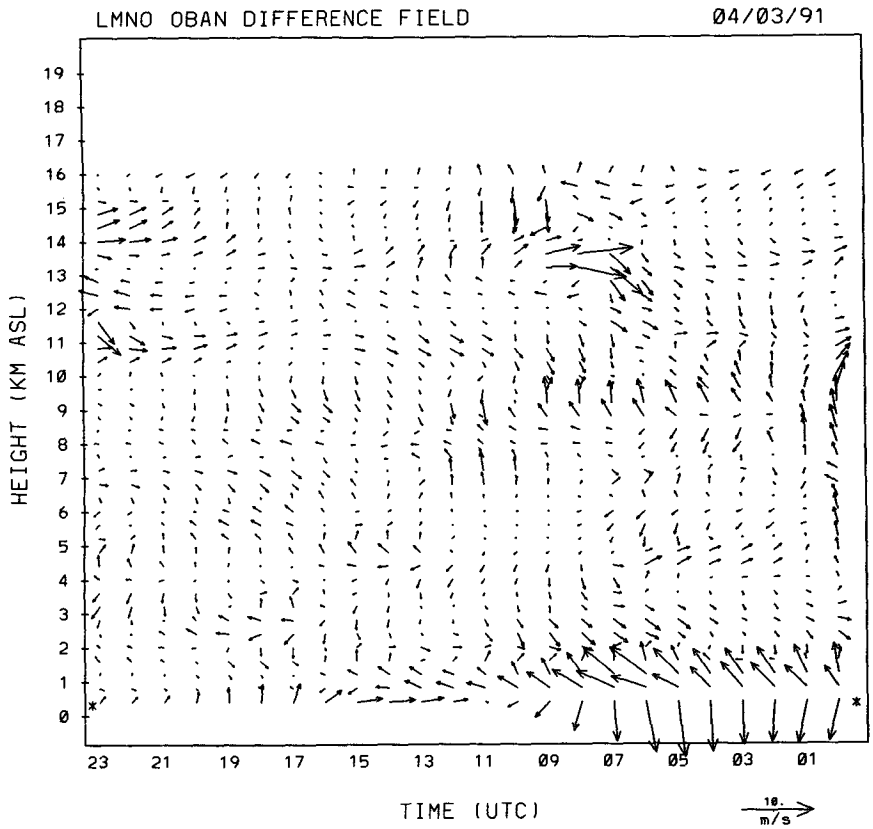

FIG. 9. The vector difference field between the Doswell and correlation method analyses for 3 April 1991 (Figs. 7a,b). Note the change in scale of the reference vector.

of the mean data sampling intervals. By not allowing poorly sampled features to contaminate the results, derivative quantities exhibit good temporal and spatial continuity. Hence, in most situations where potential mesoscale features of interest are marginally sampled by the observing system(s), the D77 approach is recommended.

One potential disadvantage arises if the sampling in one dimension is mismatched with that of another. To provide an extreme example, suppose a remote sensing system sampled the atmosphere every 10 m at hourly intervals. A literal interpretation of the D77 approach would lead to a weight function that gave very little weight to data only 100–200 m away from an analysis point even though data at this distance may be highly correlated.[2] Knowledge of the space–time structure of the sampled variable is needed to determine if this analysis behavior is desirable. The correlation tables presented by Brewster and Schlatter (1988) (recall that they are based on a one-month dataset from one site) show that profiler measurements indeed have strong correlation ±500–1000 m in the vertical from a reference point—that is, as strong as the correlation among data ±1 h from this point. Hence, the profiler may be measuring vertical structure whose behavior in time cannot be determined from hourly time resolution. This mismatch in the sampling frequencies may lead the D77 procedure, if inappropriately applied, to overfit the data in one dimension compared to another.

The correlation method borrows a concept from the optimum interpolation approach to objective analysis in that we desire to assign equal weight to data that are equally correlated in time and space. The use of time–height correlation tables produced from profiler data allows the observed statistical structure of the wind field to determine the Barnes filter parameters such that this goal is met. In this respect, the correlation method can provide anisotropic weighting of the observations if such weighting is justified by the statistics. As discussed above, this technique is recommended for use when there is a mismatch (i.e., a physical inconsistency) in the sampling intervals between two or more dimensions (usually time and one spatial direction). Disadvantages

[2] That is, we have assumed that $\lambda/\Delta s = \tau/\Delta t$ in our application of D77. We could, for example, use the space–time correlation information obtained for the correlation method to eliminate the mismatch in time and space weighting by computing an appropriate choice of the ratio of $\lambda/\Delta s$ to $\tau/\Delta t$.

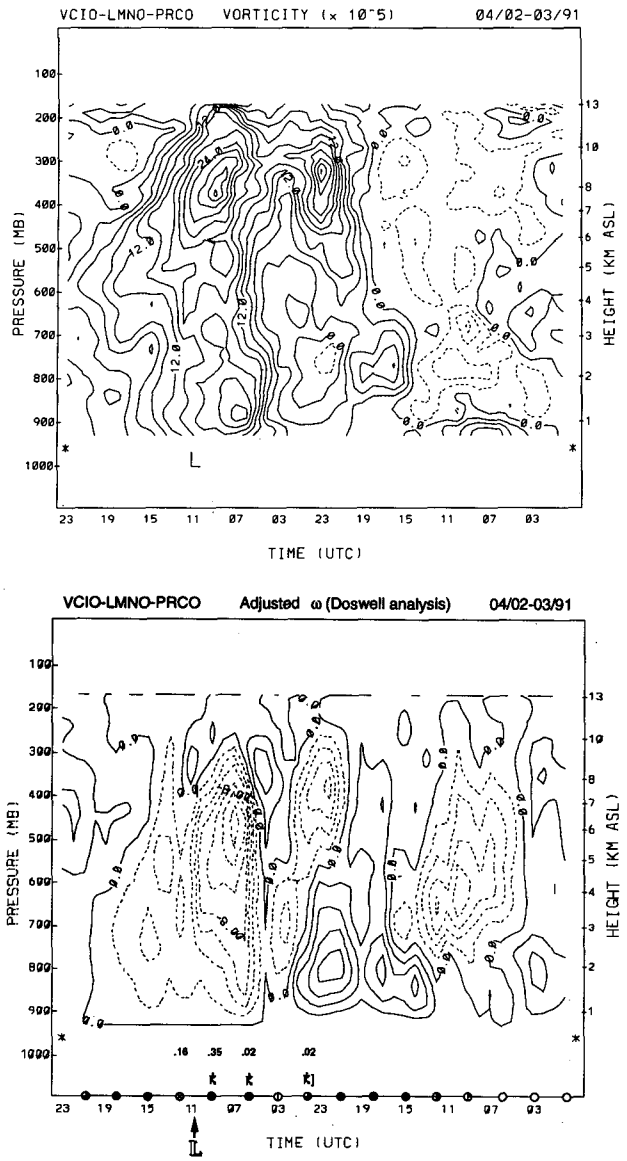

FIG. 10. Time–height section for the Vici–Lamont–Purcell profiler triangle for 0000 UTC 2 April–2300 UTC 3 April 1991 of (a) relative vorticity ($\times 10^5$ s^{-1}), contour interval 3.0 $\times$ 10^{-5} s^{-1} before scaling; and (b) vertical motion (adjusted kinematic omega), contour interval of 2.0 μb s^{-1}, from a two-pass Doswell analysis procedure. Dashed contours are negative. The "L" symbol marks the position of the surface low. Cloud cover, observed weather and 3-h precipitation amounts are indicated on the vertical motion chart.

of the correlation method include the need to compute correlation tables at different sites for different seasons, and use of these tables in weather situations that deviate significantly from the climatologically averaged statistical behavior. Correlation tables also could be determined, however, for specific weather phenomena or regimes. (Recall, though, that the sensitivity of analyses from the correlation method to spatial and temporal variations in the correlation statistics has not been examined here, and such testing is needed to determine the value of computing these statistics.)

Other observations and findings from this work include the following:

1) Unless the observations are uncommonly accurate, there is no need to use more than one pass of a Barnes-type scheme to recover the significant meteorological features in a dataset, provided the appropriate filter parameters are selected. In fact, the use of two or more passes may lead to the overfitting of the data when compared to its standard error of measurement. We used the Strauch et al. (1987) error estimates here, but if improved estimates of the errors in the WPDN

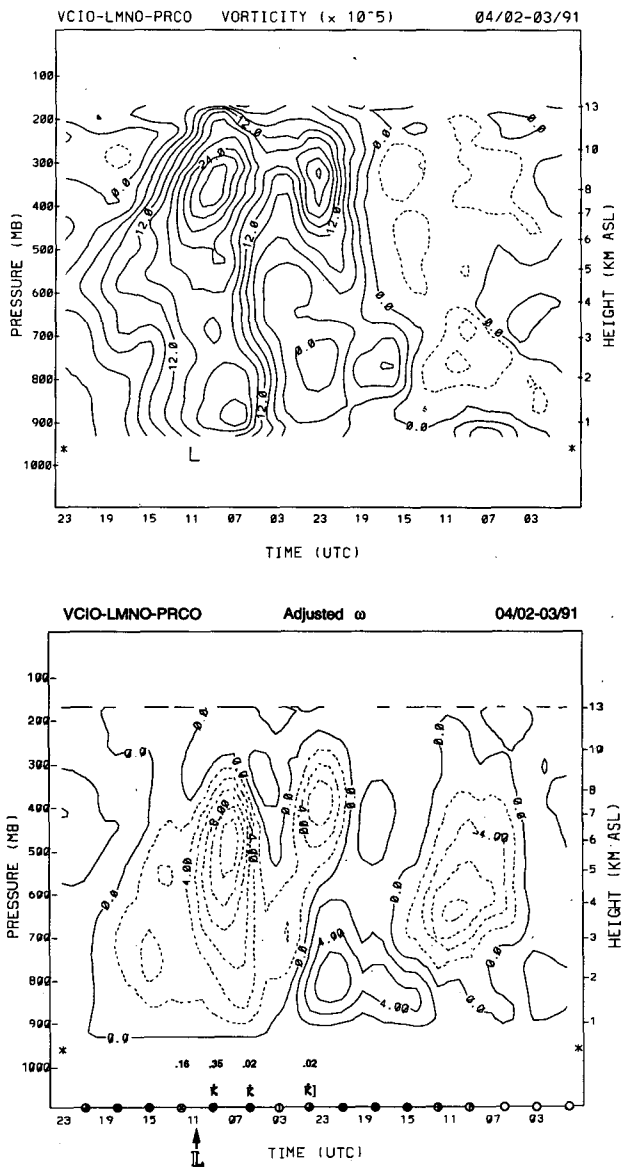

FIG. 11. Same as Fig. 10 except for a one-pass Doswell analysis procedure.

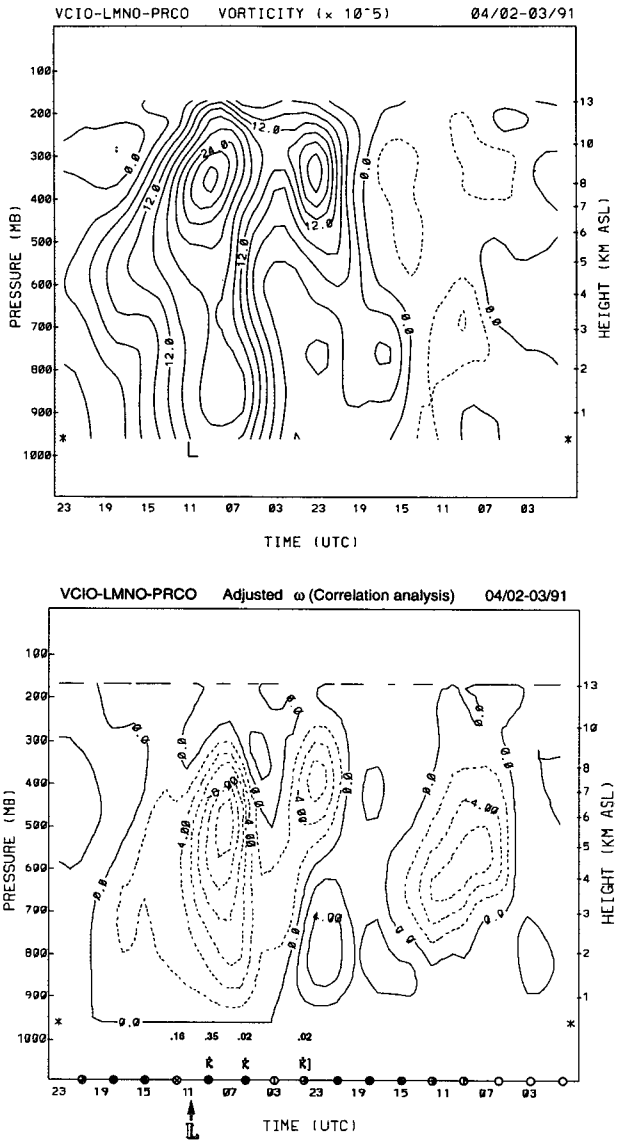

FIG. 12. Same as Fig. 10 except for a one-pass correlation method procedure.

data become available, then the analysis parameters should be adjusted accordingly.

2) Kinematic calculations computed from the objectively analyzed time–height wind fields are not very sensitive, especially with respect to the location of major features, to changes in the filter parameters. This is consistent with known properties of distance-dependent weighted analyses. For example, Thiébaux and Pedder (1987, p. 102) show that the spatial response of an interpolation process using an isotropic distance-dependent weight function is not isotropic if the observations are not distributed homogeneously. However, if the data are uniformly sampled, as is often the case with wind profiler time–height sections, distance-dependent weighting will smooth the field, reducing the amplitude of the extrema, but will not phase-shift the observed pattern (see appendix B). We noted, for example, that the vorticity and vertical motion fields from the correlation method (Fig. 12) are, as expected, even smoother than those from the one-pass D77 fields shown in Fig. 11, but the important features are still in the same space–time positions.

3) The results show (at least for the June Colorado data that provided our correlation statistics) that there is indeed a mismatch between hourly profiler data that provide vertical resolution of 250 m. A more physically consistent data presentation is the use of the 6-min profiler data that actually are produced by each WPDN system before the hourly consensus averaging takes place. In general, we recommend that correlation tables be developed from the output of any new observing system in order to determine physically consistent sampling intervals for it and future systems.

Acknowledgments. The authors wish to thank Keith Brewster for his advice during this research and Howie Bluestein for his helpful comments. We thank John Augustine, Jose Meitin, Laurie Hermes, Steve Million, and Tim Hughes for providing the data. Appreciation is expressed to Patty Miller for providing the results of two other quality control procedures from which we could evaluate the performance of our method, and for reading the manuscript. Special thanks are owed to Drs. Marty Ralph, Jim Wilczak, and Dave Stensrud for their thorough and helpful reviews of the manuscript, and especially to Dr. Ralph for providing detailed profiler spectral moment data to us. This work was completed while the first author was a visiting scientist at NOAA's Forecast Systems Laboratory; he thanks Tom Schlatter, John McGinley, and Stan Benjamin for their hospitality. This work was supported by NOAA Grant NA85RAD05040 and by NSF Grant ATM-8819619.

APPENDIX A

Kinematic Calculations

The kinematic computations are performed using the line integral method as evaluated by the linear vector point function technique of Zamora et al. (1987). We have included here the effect of the earth's curvature, which was neglected in the earlier work. Hence the linear velocity components are approximated by

$$\frac{u}{\sigma}(x, y) \approx \frac{u}{\sigma}(x_0, y_0) + \frac{\partial(u/\sigma)}{\partial x}\delta x + \frac{\partial(u/\sigma)}{\partial y}\delta y \quad \text{(A1)}$$

$$\frac{v}{\sigma}(x, y) \approx \frac{v}{\sigma}(x_0, y_0) + \frac{\partial(v/\sigma)}{\partial x}\delta x + \frac{\partial(v/\sigma)}{\partial y}\delta y, \quad \text{(A2)}$$

where σ is the image scale factor for the map projection, here chosen to be the polar stereographic value

$$\sigma = \frac{1 + \sin\phi_0}{1 + \sin\phi}, \tag{A3}$$

where ϕ is the station latitude and ϕ_0 is the standard latitude of the map projection. The point (x_0, y_0) defines the map coordinates of the triangle centroid, $\delta x = x - x_0$ and $\delta y = y - y_0$. Following Saucier (1955, p. 316), we can now define the four kinematic quantities on the image plane

$$\begin{aligned}
\text{def}\,\mathbf{V} &= 2a = \sigma^2\left[\frac{\partial(u/\sigma)}{\partial x} - \frac{\partial(v/\sigma)}{\partial y}\right] \\
\text{def}'\mathbf{V} &= 2a' = \sigma^2\left[\frac{\partial(v/\sigma)}{\partial x} + \frac{\partial(u/\sigma)}{\partial y}\right] \\
\text{div}\mathbf{V} &= 2b = \sigma^2\left[\frac{\partial(u/\sigma)}{\partial x} + \frac{\partial(v/\sigma)}{\partial y}\right] \\
\text{rot}\mathbf{V} &= 2c = \sigma^2\left[\frac{\partial(v/\sigma)}{\partial x} - \frac{\partial(u/\sigma)}{\partial y}\right].
\end{aligned} \tag{A4}$$

Use of the expressions (A4) in (A1) and (A2) yields

$$\frac{u}{\sigma} = \frac{u_0}{\sigma_0} + \frac{1}{\sigma_0^2}(a\delta x + a'\delta y + b\delta x - c\delta y) \tag{A5}$$

$$\frac{v}{\sigma} = \frac{v_0}{\sigma_0} + \frac{1}{\sigma_0^2}(-a\delta y + a'\delta x + b\delta y + c\delta x), \tag{A6}$$

where σ_0, u_0, and v_0 are the image scale factor and horizontal velocity components at the origin (triangle centroid). Writing (A5) and (A6) for each of the observed wind components at the triangle vertices, the resulting system of six equations in six unknowns can be written as

$$\mathbf{DX} = \mathbf{U}, \tag{A7}$$

where $\mathbf{D} = (u_0/\sigma_0, v_0/\sigma_0, a, a', b, c)$ is the row vector of unknowns, $\mathbf{U} = (u_1/\sigma_1, v_1/\sigma_1, u_2/\sigma_2, v_2/\sigma_2, u_3/\sigma_3, v_3/\sigma_3)$ is the row vector of observations, and

$$\mathbf{X} = \begin{bmatrix}
1 & 0 & 1 & 0 & 1 & 0 \\
0 & 1 & 0 & 1 & 0 & 1 \\
\frac{\delta x_1}{\sigma_0^2} & -\frac{\delta y_1}{\sigma_0^2} & \frac{\delta x_2}{\sigma_0^2} & -\frac{\delta y_2}{\sigma_0^2} & \frac{\delta x_3}{\sigma_0^2} & -\frac{\delta y_3}{\sigma_0^2} \\
\frac{\delta y_1}{\sigma_0^2} & \frac{\delta x_1}{\sigma_0^2} & \frac{\delta y_2}{\sigma_0^2} & \frac{\delta x_2}{\sigma_0^2} & \frac{\delta y_3}{\sigma_0^2} & \frac{\delta x_3}{\sigma_0^2} \\
\frac{\delta x_1}{\sigma_0^2} & \frac{\delta y_1}{\sigma_0^2} & \frac{\delta x_2}{\sigma_0^2} & \frac{\delta y_2}{\sigma_0^2} & \frac{\delta x_3}{\sigma_0^2} & \frac{\delta y_3}{\sigma_0^2} \\
-\frac{\delta y_1}{\sigma_0^2} & \frac{\delta x_1}{\sigma_0^2} & -\frac{\delta y_2}{\sigma_0^2} & \frac{\delta x_2}{\sigma_0^2} & -\frac{\delta y_3}{\sigma_0^2} & \frac{\delta x_3}{\sigma_0^2}
\end{bmatrix}$$

is the coefficient matrix, which is constant for a given triangle. Solution of (A7) for $\mathbf{D}$ yields not only the four kinematic quantities defined in (A4) but also the mean or translational wind components (u_0, v_0) over the triangle.

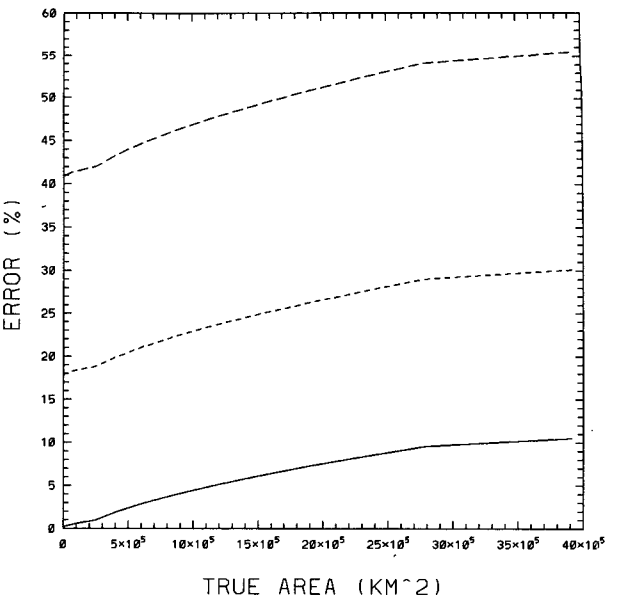

FIG. A1. Percent error between triangles computed with and without earth curvature effects as a function of standard latitude and triangle size. The solid, short-dashed, and long-dashed lines are for ϕ_0 = 35.9°, 45°, and 60° latitude, respectively.

The question, "At what triangle size should earth curvature effects be taken into account?" naturally arises. To answer this, we computed the percent error between triangles computed with and without curvature effects as a function of the standard latitude ϕ_0 used in the map projection formula (A3). As can be seen in Fig. A1, the effect of not using a standard latitude near the centroid of the triangle is much larger than the effect of size. If ϕ_0 is defined at the centroid (solid line in Fig. A1), then curvature errors do increase with triangle size but remain less than 10%. However, if one desires to perform calculations on the same image plane over a large portion of the profiler network, significant errors arise just 10°–15° latitude away from ϕ_0. Given the ease of including the curvature effect in equations (A4) and (A7), we recommend that it become standard practice.

APPENDIX B

Distance-Dependent Weighted Averaging and Phase

For simplicity, we shall treat the problem in one dimension. Assume the observations are given by $\hat{f}(\hat{x}_i)$, where the sample points $\hat{x}_i = \hat{x}_o + i\Delta\hat{x}$ define a uniform mesh of observation points, and $i = 1, 2, \cdots, N$, where N is some integer. In what follows, the issues associated with data domain boundaries will be ignored; for a

treatment of boundary effects, see Pauley (1990). The task of objective analysis (i.e., mapping the observations from their original locations to the points x_j) will be accomplished by a distance-dependent weighted average (DDWA) of surrounding observations, according to

$$f(x_j) = \frac{\sum_{i=1}^{N} \hat{f}(\hat{x}_i) w(|x_j - \hat{x}_i|)}{\sum_{i=1}^{N} w(|x_j - \hat{x}_i|)}, \quad \text{(B1)}$$

where w is a weighting function that depends on the distance $|x_j - \hat{x}_i|$. As discussed in Doswell and Caracena (1988), the denominator in (B1), which they called the *normalizing factor,*

$$W_j \equiv \sum_{i=1}^{N} w(|x_j - \hat{x}_i|), \quad \text{(B2)}$$

can be a problem if it varies significantly in space. Here, however, any such spatial variation is ignored, implying that both data and analysis points are uniformly distributed. Under this assumption, W_j is everywhere constant ($=W$) so that (B1) can be rewritten as

$$f(x_j) = \sum_{i=1}^{N} \hat{f}(\hat{x}_i) \omega(|x_j - x_i|),$$

where

$$\omega(|x_j - x_i|) = \frac{w(|x_j - x_i|)}{W},$$

is the *normalized* weighting function.

Let $\hat{F}(k_j)$ denote the Fourier transform of the original data (where k is wavenumber), F denote the Fourier transform of the analyzed field, and W that of the normalized weighting function. Objective analysis by DDWA can be considered a form of convolution[3] [see Blackman and Tukey (1958, p. 72)], and we shall denote the convolution operator with an asterisk. The convolution theorem asserts that if $f = \hat{f} * \omega$, then $F = \hat{F}\Omega$; that is, the transform of a convolution is the product of transforms.

The original spectrum can be expanded into real and imaginary parts

$$\hat{F} = \hat{F}_r + i\hat{F}_i, \quad \text{(B3)}$$

where $i = (-1)^{1/2}$, and subscripts r and i denote real and imaginary parts, respectively, and the original spectrum also can be expressed as

$$\hat{F}(k) = |\hat{F}| e^{i\hat{\varphi}k}. \quad \text{(B4)}$$

It follows from this expansion, then, that the phase of the original function is given by

$$\hat{\varphi} = \tan^{-1}\left(\frac{\hat{F}_i}{\hat{F}_r}\right),$$

while that of the objectively analyzed function is, using $F = \hat{F}\Omega$, (B3), and (B4),

$$\varphi = \tan^{-1}\left(\frac{\hat{F}_i\Omega_r + \hat{F}_r\Omega_i}{\hat{F}_r\Omega_r - \hat{F}_i\Omega_i}\right). \quad \text{(B5)}$$

Therefore, inspection of (B5) shows that if Ω_i vanishes, the phase of the analyzed function will be the same as that of the original data. In one dimension, Ω_i vanishes when the weighting function is *even.* For two dimensions, this requirement means that the weighting function is *isotropic.* Hence, isotropic weighting introduces no phase shift. Note that when the weighting is isotropic, the absolute value can be dropped from the argument of the weighting function in the foregoing.

As already observed, this derivation is contingent on the uniformity of the normalizing factor. Whenever the data are not uniformly distributed, the normalizing factor will not be constant (although for some purposes and in some situations, its variation can be neglected). Therefore, we anticipate the possibility of phase shifts associated with DDWA near data domain boundaries (as noted in Pauley 1990), and even within the interior of data domains that have significant clustering and/or data voids.

[3] In this case, the transform is discrete, although it can be treated with continuum mathematics using the artifice of convolving a hypothetical continuous function with a Dirac comb, as in Pauley and Wu (1990).

REFERENCES

Achtemeier, G. L., 1989: Modification of a successive corrections objective analysis for improved derivative calculations. *Mon. Wea. Rev.,* **117,** 78–86.

Barnes, S. L., 1964: A technique for maximizing details in numerical weather map analysis. *J. Appl. Meteor.,* **3,** 396–409.

——, 1973: Mesoscale objective map analysis using weighted time-series observations. NOAA Tech. Memo. ERL NSSL-62, Norman, OK, 60 pp.

Blackman, R. B., and J. W. Tukey, 1958: *The Measurement of Power Spectra.* Dover Publications, Inc., 190 pp.

Brewster, K. A., 1989: Wind Profiler Training Manual #2—Quality Control of Wind Profiler Data. NOAA/ERL/FSL, 39 pp. [Available from Demonstration Division-Profiler Program, NOAA/ERL/FSL, 325 Broadway, Boulder, CO.]

——, and T. W. Schlatter, 1986: Automated quality control of wind profiler data. Preprints, *11th Conf. on Weather Forecasting and Analysis,* Kansas City, KS, Amer. Meteor. Soc., 171–176.

——, and ——, 1988: Recent progress in automated quality control of wind profiler data. Preprints, *Eighth Conf. on Numerical Weather Prediction,* Baltimore, MD, Amer. Meteor. Soc., 331–338.

Doswell, C. A., III, 1977: Obtaining meteorologically significant surface divergence fields through the filtering property of objective analysis. *Mon. Wea. Rev.,* **105,** 885–892.

——, and F. Caracena, 1988: Derivative estimation from marginally sampled vector point functions. *J. Atmos. Sci.,* **45,** 242–253.

Koch, S. E., M. DesJardins, and P. J. Kocin, 1983: An interactive Barnes objective map analysis scheme for use with satellite and conventional data. *J. Climate Appl. Meteor.*, **22,** 1487–1503.

Pauley, P. M., 1990: On the evaluation of boundary errors in the Barnes objective analysis scheme. *Mon. Wea. Rev.*, **118,** 1203–1210.

——, and X. Wu, 1990: The theoretical, discrete, and actual response of the Barnes objective analysis scheme for one- and two-dimensional fields. *Mon. Wea. Rev.*, **118,** 1145–1163.

Saucier, W. J., 1955: *Principles of Meteorological Analysis.* The University of Chicago Press, 438 pp.

Schaefer, J. T., and C. A. Doswell III, 1979: On the interpolation of a vector field. *Mon. Wea. Rev.*, **107,** 458–476.

Spencer, P. L., 1992: Diagnosis of a decaying baroclinic wave using a network of wind profilers. M.S. thesis, Univ. of Oklahoma, 105 pp. [Available from the School of Meteorology, University of Oklahoma, Norman, OK 73019.]

Strauch, R. G., B. L. Weber, A. S. Frisch, C. G. Little, D. A. Merritt, K. P. Moran, and D. C. Welsh, 1987: The precision and relative accuracy of profiler wind measurements. *J. Atmos. Oceanic Technol.*, **4,** 563–571.

Thiébaux, H. J., and M. A. Pedder, 1987: *Spatial Objective Analysis.* Academic Press, 299 pp.

Wilczak, J. M., R. G. Strauch, F. M. Ralph, B. L. Weber, D. A. Merritt, J. R. Jordan, D. E. Wolfe, L. K. Lewis, D. B. Wuertz, J. E. Gaynor, S. A. McLaughlin, R. R. Rogers, A. C. Riddle, and T. S. Dye, 1995: Contamination of wind profiler data by migrating birds: Characteristics of corrupted data and potential solutions. *J. Atmos. Oceanic Technol.*, **12,** 449–467.

Zamora, R. J., M. A. Shapiro, and C. A. Doswell III, 1987: The diagnosis of upper tropospheric divergence and ageostrophic wind using profiler wind observations. *Mon. Wea. Rev.*, **115,** 871–884.